Eur Food Res Technol (2013) 237:639–646
DOI 10.1007/s00217-013-2022-x

ORIGINAL PAPER

Determination of oxygen transmission barrier of microcapsule wall by crocetin deterioration kinetics

Hui Zhou · Xiaofan Yuan · Qingsheng Zhao · Bing Zhao · Xiaodong Wang

Received: 1 February 2013 / Revised: 2 April 2013 / Accepted: 22 April 2013 / Published online: 19 June 2013
© Springer-Verlag Berlin Heidelberg 2013

Abstract Microencapsulation was a widely used technique for the unstable materials because the wall prevented the core from contacting with oxygen. To improve the stability of crocetin and maximize the protection afforded by the wall, in the present study, microencapsulation was applied for crocetin by spray-drying the first time with three wall materials (beta-cyclodextrin, gum arabic and maltodextrin). The oxygen transmission barrier was proposed to evaluate the potential gas barrier of these wall materials, and it was measured by the deterioration kinetics of crocetin. To enhance the oxygen transmission barrier of the wall, the major conditions of spray-drying and the storage were investigated. Results showed that the deterioration rate followed the first kinetic model closely. Spray-drying was applicable to microencapsulating crocetin with the microencapsulation efficiency of 77.91–85.03 % under the inlet air temperature 210 °C. The oxygen pressure in the microcapsule was reduced to $<0.114 \pm 0.005$ atm for all the three wall materials. The oxygen transmission barrier of the wall microencapsulated by the three materials was qualified by thermodynamic parameter activation energy (29.436 ± 0.080, 58.813 ± 0.312 and 49.376 ± 0.125 kJ/mol, respectively). Gum arabic was the most suitable agent for microencapsulating crocetin, and a dry environment was preferred for its storage because the low relative humidity was beneficial to the stable structure of the microcapsule. This study would be helpful to the industrial application of crocetin.

H. Zhou · X. Yuan (✉) · Q. Zhao · B. Zhao · X. Wang
Zhongguancun, No. 1 Bei er tiao, Haidian District, Beijing 100190, People's Republic of China
e-mail: xfyuan@home.ipe.ac.cn

Keywords Activation energy · First order kinetics model · Microencapsulation · Oxygen pressure · Spray-drying

Introduction

Crocetin (CT) is a precious bioactive substance which is majorly responsible for the medicine efficacy of such herbals as stigma of saffron and the fruit of gardenia. Most of the CT-glycosylated derivatives also show great pharmacological activities [12, 26]. This biological function may be typically determined by the conjugated skeleton composed of 20 carbon atoms shown in Fig. 1 [22]. Unfortunately, the unsaturated molecular structure can also play a bad role in the stability during the handling process and storage. This instability is affected by many factors such as temperature, pH and ionic strength on the physical and chemical stability [14]. For a simple but reasonable principle, the access degree to oxygen can be considered as the most important factor determining the self-deterioration of the unstable conjugated skeleton in the in vitro study [8]. Keeping away the oxygen from CT is a good strategy for the CT storage.

Many methods were proposed to slow down the self-deterioration of those bioactive substances. Microencapsulation was widely used to prolong the storage time of unstable additives such as essential oils, flavors and carotenoids [5, 19]. Different wall materials provided the core protection with different strength from the oxygen or moisture due to their ability of shielding the bioactive substance. Spray-drying was a preferred technique yielding microencapsulated powder because of the low cost, and the choice of wall material was the key step. The microencapsulation efficiency, stability under different storage conditions, and degree of protection provided to the core

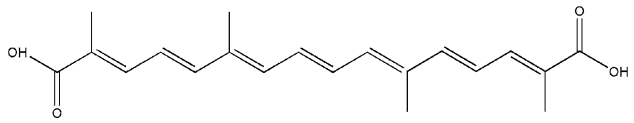

Fig. 1 The structure of crocetin ($C_{20}H_{24}O_4$, Mr = 324 Da)

material were evaluated and the surface morphology was observed by scanning microscopy. Wagner and Warthesen [23] pointed out that compared with the 2 days half-life of the carrot juice spray-dried alone, carotenes microencapsulated with 36.5 dextrose equivalent hydrolyzed starch had a predicted half-life of 450 days at 21 °C. The half-time of cumin oleoresin extended to more than twice by microencapsulation with a blend of gum arabic, maltodextrin and modified starch [7]. Another author Wang et al. [24] showed that the stability of lutein microencapsulated with a mixture wall material against heat, pH, light and oxygen was also greatly improved and their retention rates had been improved about 15–50 % than that of free lutein.

Many literatures reported the spray-dry process and the consequent kinetic study [1, 2, 15] aiming at obtaining high microencapsulation efficiency and improving the stability of the bioactive components, such as saffron carotene and carotene. Tsimidou and Biliaderis [20] pointed out that the carotene deterioration followed the first order kinetic model. Selim et al. [18] discussed the deterioration of saffron water-soluble carotenoids (mainly crocins) microencapsulated by freeze-drying, and results showed that the polymeric matrices used as wall materials largely decreased the oxidation rates of CT glycosides. This improvement should be attributed to the dilution and dispersion of the CT glycosides into the powder because of the water-soluble core tending toward the amorphous matrices rather than the hollow wall-embedding structure. However, it was not the powder but the wall formed in spray-drying that deserved the attention due to protecting the core.

In this article, the wall rather than the spray-drying powders in many literatures was focused and the oxygen transmission barrier was proposed in order to qualify the quality of the wall. The water-insoluble core CT was microencapsulated in hollow structure with the common wall materials: beta-cyclodextrin (BC), gum arabic (GA) and maltodextrin (MD) by spray-drying. The oxygen pressure (OPR) in the microcapsule was measured based on the detailed stability study of the spray-dried CT and the effects of the spray-drying. The effects of storage conditions on OPR were also investigated and optimized to reduce the gas entrance. The activation energy was used for evaluating the quality of the wall. This work was beneficial for choosing the best wall material and the preferred storage conditions for CT.

Materials and methods

Materials

Analytically pure hexane was supplied from West Long Chemical Co., Ltd, China. BC, GA and MD were supplied from Sinopharm Chemical Reagent Co., Ltd, China. Analytically pure methanol and analytically pure *N*,*N*-dimethylformamide were supplied from Sinopharm Chemical Reagent Co., Ltd, China. The CT reference substance with the purity up to 96 % was self-prepared in our laboratory.

The measurement of CT content

In brief, CT content in the microencapsulated powder was determined with the similar method described by Desobry et al. [3], and it was expressed by the following equation:

$$R_{CT} = f \times (A/E). \quad (1)$$

where R_{CT} is CT content, A is absorbance value; $E = 252.0$, which is the extinction coefficient of CT at $\lambda_{max} = 421$ nm when methanol is used as solvent; f is dilution multiple measured by volume.

In order to obtain the CT content entrapped in the microcapsule, total CT content (the proportion of CT in the microencapsulated powder) and surface CT (the CT content attached to the powder) were measured. Total CT content: 0.01 g of CT microencapsulated powder was put in an empty brown vial, into which 1 mL *N*,*N*-dimethylformamide was added to break the wall of the powder. Then 10 mL methanol was pipetted into the vial. The vial was shaken at 60 rpm for 1 h. The solution was then filtered by a 0.21-μm membrane filter and analyzed with ultraviolet spectrophotometer. Surface CT content: 0.01 g CT microencapsulated powder was put in an empty brown vial, into which 1 mL hexane was added to extract the surface CT of the powder. The vial was shaken at 60 rpm for 1 h. The operation was repeated five times until the hexane fraction turned transparent and all the fractions were mixed then the solvent hexane was evaporated and CT was redissolved in 10 mL methanol. The solution was then filtered by a 0.21-μm membrane filter and analyzed with ultraviolet spectrophotometer.The CT entrapped in the capsule was the difference between the total CT and the surface CT.

$$CT_{Entrapped} = CT_{Total} - CT_{Surface}. \quad (2)$$

Additionally, the microencapsulation efficiency (EE) can be calculated by the following equation:

$$EE = \frac{CT_{Total} - CT_{Surface}}{CT_{Total}} \times 100\,\% \quad (3)$$

CT microencapsulation

Three wall materials, BC, GA and MD were used for the preparation of emulsions, and the liquid–solid ratio were 5:1, 10:1 and 15:1. Nine kinds of emulsions were prepared by the combination of liquid–solid ratio and the wall category.

Wall materials were dissolved with pure water in a 1-L plastic jar. After the wall materials completely dissolved, the plastic jar was immersed in a cold water bath for 10–20 min until the temperature reached 10–12 °C. CT was added and the emulsions were stirred at 8,000 rpm for 2–3 min. The coarse emulsions were then homogenized using a homogenizer (APV, Germany) at 100 atm for 15 min.

The emulsions were pumped into the spray-dryer (YC-015, Shanghai Pilotech Instrument & Equipment Company Ltd, China) chamber at a constant flow rate of 60 mL/min and the outlet temperatures were kept at 85 ± 5 °C. CT microencapsulated powder was transferred immediately into a cold glass jar.

Storage conditions

Powder samples (2 g of each) were placed in a narrow-mouth glass bottle and covered with aluminum crimp seal. These bottles were stored for 10 days at 35 °C in the exposure of natural light, and the relative humidity (RH) was 0.75. The RH was kept by NaCl saturated solutions as the literature [9] listed. The measurement was repeated in triplicate. The change of CT content with time was critically calculated.

The morphology analysis of the microencapsulated powder

The microcapsule was attached to scanning electron microscope stubs using two-sided adhesive tape. The specimens were coated with gold under vacuum condition at 5 kV, and then observed on a Hitachi-2150 scanning electron microscope (SEM, Japan) for evaluation of the morphology.

The deterioration kinetic model

The first kinetic model of CT deterioration can be expressed by the following equation. A semi-log plot of percentage retention of CT content versus time was plotted by six data points to obtain the deterioration rate constant (k) as the slope of the graph.

$$\mathrm{Ln}(C/C_0) = k \times t \tag{4}$$

where C is the CT content after deterioration; C_0 is the initial CT content; k is the first order deterioration rate constant calculated from deterioration time slope and t is the storage time (days). Accordingly, the half-time can be obtained as the following equation.

$$t_{1/2} = -0.693/k \tag{5}$$

where half-time $t_{1/2}$ is the storage time (days) to which the initial CT concentration turns to half and k is the kinetic deterioration rate constant.

The calculation of OPR of the microcapsule

It was assumed that the CT deterioration was dependent on the surrounding OPR of CT and, the wall slowed the deterioration by reducing the OPR. OPR can be calculated by the deterioration rate constant k value, and this is expressed by the following equation.

$$P(\mathrm{O}_2) = \frac{k - k_0}{k'} \tag{6}$$

where $P(\mathrm{O}_2)$ is the oxygen pressure in microcapsule (atm); k is the first order deterioration rate constant (day^{-1}) of the internal CT; Before finding out the mathematical relation of OPR–k, two related CT deterioration parameters were estimated.

The natural deterioration rate constant (k_0, day^{-1}) means the intercept of the OPR–k plot and, it was the slope calculated by Eq. (4) when the CT powder was put under the vacuum condition (OPR = 0 atm).

The natural deterioration rate constant (k_1, day^{-1}) is the CT deterioration rate constant, and it was calculated by Eq. (4) when the CT powder was put under the atmospheric environment and the OPR was set as 1/5 atm (OPR = 1/5 atm) according to the proportion of oxygen in the air.

The coefficient k' ($\mathrm{day}^{-1}\ \mathrm{atm}^{-1}$) represents the slope of the OPR–k plot, and it was calculated when k_1 and k_0 were put in Eq. (6).

The activation energy of the oxygen transmission rate

In order to screen the most suitable wall material for lipid microencapsulation, a quantitative method based on the activation energy of oxygen transmission rate had been proposed. E_a indicated the extra energy needed for driving a kinetic process in thermodynamics. Arrhenius law described this relationship of the kinetic rate and the temperature [13]. A plot of natural logarithm of kinetic rate versus $1/T$ yields a straight line with slope $-E_a/R$, where E_a is in kJ/mol. The oxygen transmission rate of the wall was positive related to the OPR. So this method was used to measure E_a similarly but with an improved formation as following equation:

$$\mathrm{Ln}\frac{P(\mathrm{O_2})_1}{P(\mathrm{O_2})_2} = -\frac{E_a}{R}(1/T_2 - 1/T_1) \quad (7)$$

where $P(O_2)_1$ (atm) and $P(O_2)_2$ (atm) are the OPR in microcapsule with the storage temperature T_1 (K) and T_2 (K) correspondingly. E_a is the activation energy of the oxygen transmission barrier (kJ/mol). R is the molar gas constant, 8.314 $J{\cdot}mol^{-1}{\cdot}K^{-1}$.

Experimental design and statistical analysis

The effect of the spray-drying inlet air temperature, the liquid–solid ratio of the emulsions and the storage relative humidity on the OPR were investigated. The statistical analysis was done using Statistics Analyses Systems version 9.2, and experimental data were obtained by the methods discussed above. All graphs were created using OriginPro (OriginLab Operation, Northampton, MA-USA).

Results and discussion

The spray-drying process

Figure 2 shows the morphology of the microcapsule. The surface of the microencapsulated powder was concave and shriveled, which had typical characteristics of microcapsule produced by spray-drying [25]. Nijdam and Langrish [11] described the mechanisms that the concave was formed due to the appearance of a "vacuole" inside the particles immediately after the crust development. When the particle temperature exceeded the water boiling point and the vapor pressure within the vacuole rose above the local ambient pressure, this crust inflated but contracted accordingly when the vapor was dissipated. Then, the concave formed on the surface of the particles and the difference between the high external pressure and low internal pressure of the wall sustained the concave. There was no crack on the surface which indicated that the three materials, BC, GA and MD were suitable agents for microencapsulating CT by spray-drying.

The EE was affected by the inlet air temperature and the liquid–solid ratio of the emulsions (data not listed). Different wall materials entrap CT with significantly different EE value. EE values of CT microencapsulated with BC, GA and MD were 78.24 ± 1.60, 85.03 ± 1.35 and 77.91 ± 1.94 %, respectively, under the inlet air temperature 210 °C and the liquid–solid ratio 10:1. These EE values of the CT microencapsulated powder were somewhat higher than those of the β-carotene and lycopene microencapsulated by starch [10, 16]. GA was the primary wall material for microencapsulating CT according to the EE. Comparing with the saffron carotene derivatives dissolving in water to prepare the emulsions, CT was kept particle formation the whole process that formed the definite wall/core microcapsule structure.

The kinetic of CT deterioration and the OPR in the microcapsule

The conjugated bonds of CT can be saturated by oxygen, and there was no new characteristic absorption peak before and after 3 days storage, but the peek strength is changed as shown in Fig. 3.

Figure 4 shows that the variation of CT content with storage time gave a better mathematical fit when the first order kinetics model was used ($R^2 > 0.9$). The CT powder deteriorated fast, and the microencapsulated powder with GA wall can slow down the deterioration efficiently.

The CT nature deterioration rate constant is presented in Table 1. CT itself had a half-time as long as 33 days without the existence of oxygen; however, oxygen shorted this period almost to 9 %, which quantified the assumption that the oxygen was a key factor affecting the CT deterioration. Storage temperature was another factor that changed the deterioration rate constant as the most reactions. This accorded with the experimental observation of the red color fading of the powder. Compared with the other two materials, GA wall had the lowest mass transfer coefficient of oxygen, which indicated the lowest OPR in microcapsule.

Table 2 shows the kinetic deterioration of the CT microencapsulated by the wall materials. The storage temperature had an influence on the deterioration. High temperature can accelerate the deterioration process by improving the kinetic rate as the most chemical reaction. What's more, all the wall helped improving the stability of CT and the half-time was prolonged into 1.65, 4.29 and 2.79 times at 35 °C. This was achieved by isolating the oxygen from the environment and keeping the surrounding oxygen at a low concentration. However, these walls varied enormously in terms of changing the deterioration rate constant. Different walls decreased the deterioration rate constant with statistical significance. GA and MD wall exhibited more exciting protection for CT than BC group because of the better performance in keeping the low OPR value of the microcapsule. Though the explanation for this is unclear, GA, which is composed of a highly branched arrangement of the simple sugars (galactose, arabinose and rhamnose) and glucuronic acids and contains a protein component (~2 % w/w) covalently bound within its molecular arrangement, was better material than the carbohydrate material in forming film microencapsulating the carotene core [21].

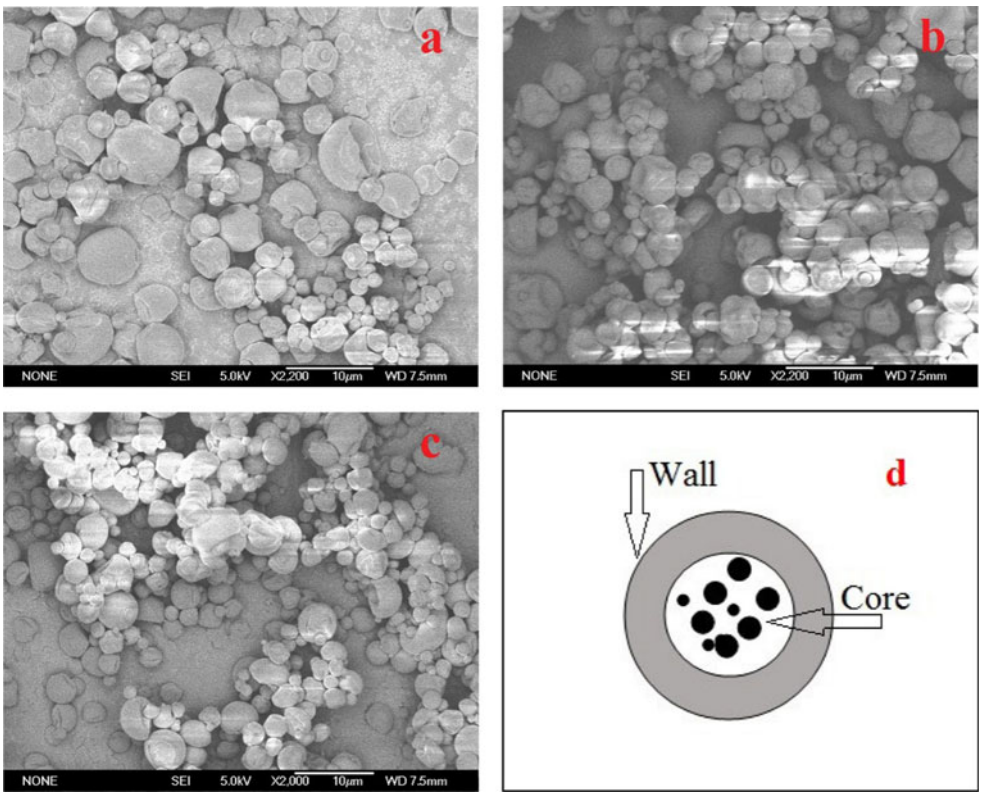

Fig. 2 The morphology of the powder of different wall materials yielded by spray-drying at 210 °C with the liquid–solid ratio of the emulsions 10:1. **a** Beta-cyclodextrin. **b** Gum arabic. **c** Maltodextrin. **d** The model of microcapsule

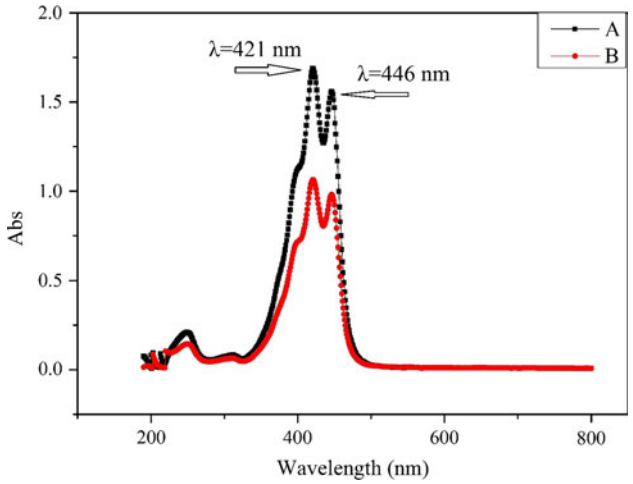

Fig. 3 The absorption curves were obtained with methanol as solvent at a concentration of 6.35 mg/L. *Curve A* turned to *curve B* after 3 days under 35 °C, relative humidity 0.75

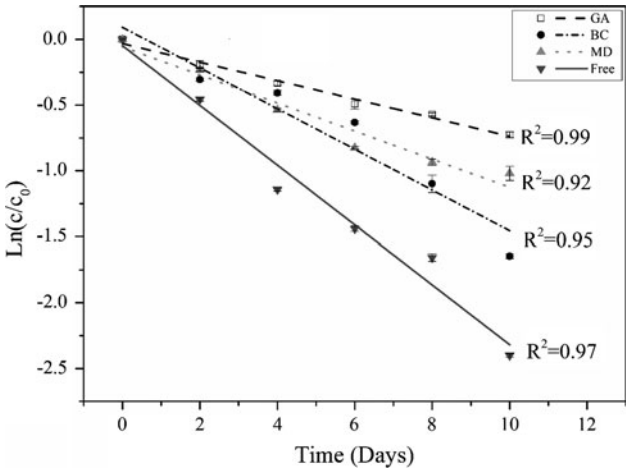

Fig. 4 The deterioration rate of crocetin in microcapsule under 35 °C and relative humidity 0.75

The factorial analysis of OPR of the microcapsule

Figure 5 shows that the OPR was markedly affected by RH. When RH increased from 0.43 to 0.75, the OPR in GA and MD microcapsule increased more than that of the BC group. For GA and MD group, the difference of OPR caused by storage relative humidity was statistically significant. The good hydroscopic property may bring GA and MD walls moisture absorption, and then, the oxygen was more permeable into the inner microcapsule, resulting in the change of the oxygen transmission barrier of the wall. So the CT microencapsulated powder should be kept in a dry environment during handling and storage.

The forming condition of the wall also played an important role in affecting the OPR in the microcapsule. When the inlet air temperature was set 210 °C, with the liquid–solid ratio of the emulsions increasing from 5:1 to 15:1, the OPR of BC, GA and MD microcapsule rose from

Table 1 The kinetic parameter of the crocetin deterioration at relative humidity 0.75

T/ °C	k_1/ $(day^{-1})^a$	$t_{1/2}$/ $(days)^b$	k_0/ $(day^{-1})^c$	$t_{1/2}$/ $(days)^d$	$k'/(days^{-1} atm^{-1})^e$
35	0.232	2.99	0.021	33.00	1.055
45	0.260	2.66	0.024	28.90	1.190

[a] The natural deterioration rate constant under the atmospheric environment when the oxygen pressure was set as 1/5 atm

[b] The half-time of CT kinetic deterioration when the oxygen pressure was set as 1/5 atm

[c] The natural deterioration rate constant under the vacuum condition when the oxygen pressure was set as 0 atm

[d] The half-time of CT kinetic deterioration when the oxygen pressure was set as 0 atm

[e] The slope of the OPR–k plot

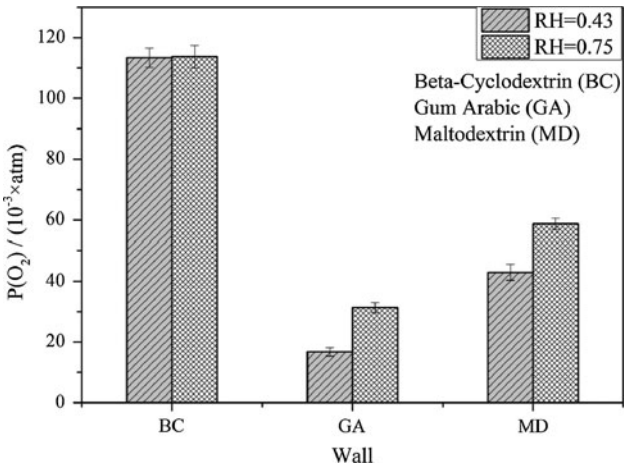

Fig. 5 Oxygen pressure in microcapsule under different relative humidity

0.101 ± 0.002, 0.027 ± 0.003 and 0.053 ± 0.003 atm to 0.118 ± 0.003, 0.035 ± 0.001 and 0.065 ± 0.003 atm, respectively, at 35 °C and RH 0.75 as shown in Fig. 6a. The data was not statistically significant but the changes of OPR indicated the liquid–solid ratio of the emulsions was an important factor. This could be explained by the oxygen transmission rate. More solid content in the emulsions with liquid–solid ratio 5:1 led to the high viscosity of the emulsions preparing for the spray-drying, which endowed the microencapsulated powder with bigger size and thick wall increasing the transmission distance for oxygen [4, 17]. Hence, the OPR in the microcapsule decreased.

Figure 6b indicates that when the inlet air temperature rose from 180 to 210 °C, the OPR exhibited a downward trend, which indicated that the oxygen transmission barrier of the wall was strengthened with an increasing inlet air temperature. This agreed with the description of the wall-forming process [6]. In fact, the water content of the powder formed by spray-drying decreased rapidly as temperature increased at a certain drying rate, which meant a rapid formation of a dense skin and a good protection against oxygen transfer into the core, resulting in lightening CT deterioration.

These discussions of the factors changing OPR showed that the oxygen transmission barrier of the wall was determined by not only the spray-drying conditions but also the conditions of the storage and relative humidity. This study on the quality of the wall was rarely reported in the literature studying the spray-drying technology alone for the purpose of the stability improvement.

Activation energy (E_a) for the oxygen transmission rate

The positive values of E_a meant that oxygen transmission rate increased with the increase in temperature, and absolute value meant the oxygen needed to absorb the equivalent power for traveling through wall. The higher the value was, the more excellent the barrier of the wall was. E_a was a comprehensive parameter related both the spray-drying and the storage. At storage RH 0.75, the highest E_a value of 58.81 kJ/mol proved that GA wall had the highest oxygen transmission barrier compared with the other two walls as

Table 2 The deterioration rate of crocetin and the oxygen pressure in the microcapsule

Wall[a]	k/$(days^{-1})^b$		$t_{1/2}$/$(days)^c$		$P(O_2)/(atm)^d$	
	35 °C	45 °C	35 °C	45 °C	35 °C	45 °C
BC	0.141 ± 0.004^A	0.217 ± 0.013^A	4.92 ± 0.09	3.19 ± 0.03	0.113 ± 0.005	0.182 ± 0.008
GA	0.054 ± 0.020^B	0.101 ± 0.006^B	12.83 ± 0.12	6.68 ± 0.11	0.034 ± 0.010	0.077 ± 0.012
MD	0.083 ± 0.011^C	0.151 ± 0.050^C	8.35 ± 0.05	4.59 ± 0.07	0.057 ± 0.007	0.122 ± 0.017

A, *B* and *C* different letters indicate significant difference at $p < 0.05$

[a] The powder was yielded by spray-drying at 210 °C, liquid–solid ratio 10:1 and then were kept at relative humidity 0.75

[b] The kinetic deterioration rate constant of the CT in the microcapsule

[c] The half-time of CT kinetic deterioration

[d] The oxygen pressure in the microcapsule

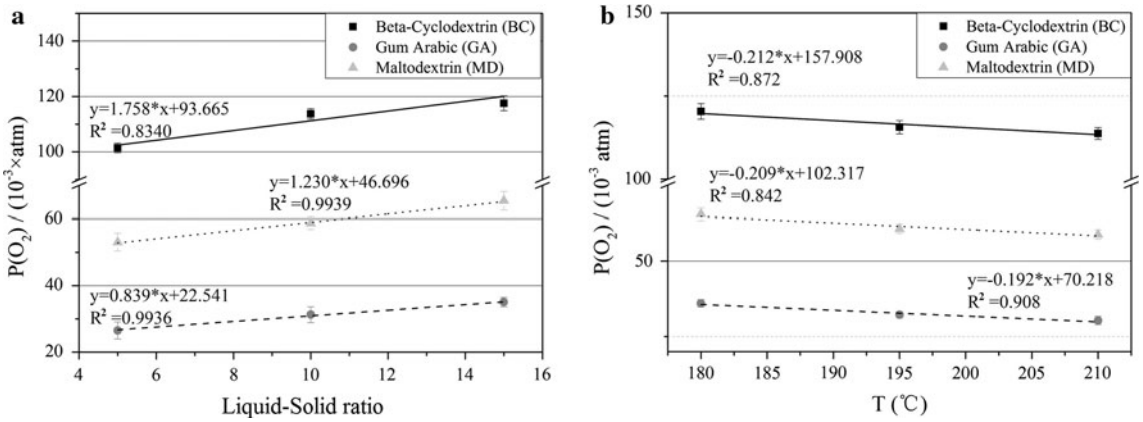

Fig. 6 The effect of spray-drying condition on oxygen pressure in microcapsule. **a** Liquid–solid ratio of the emulsions. **b** The *inlet* air temperature. The powder was kept at 35 °C and relative humidity 0.75

Table 3 The activation energy of the oxygen transmission barrier of the wall

Wall[a]	BC	GA	MD
E_a/(kJ/mol)[b]	29.448 ± 0.080	58.847 ± 0.312	49.391 ± 0.125

[a] The powder was yielded by spray-drying at 210 °C, liquid–solid ratio 10:1 and then were kept at relative humidity 0.75

[b] The activation energy of oxygen transmission barrier

shown in Table 3. Briefly, in GA wall, dry and cold condition can bring CT a much longer half-time, which was beneficial for the wide application of CT. This was in accordance with the criterion of OPR.

Conclusions

CT deterioration followed the first kinetic model with good fitness. CT can be used as a core by spray-drying, and BC, GA and MD were good wall agents for improving the stability of CT. The microencapsulation efficiency reached 77.91–85.03 %, respectively, and GA had the strongest oxygen transmission barrier, with E_a 58.813 ± 0.312 kJ/mol, that is why the OPR in GA microcapsule could be kept at a lowest level. A dry and cold environment can enhance this protection. It was revealed that the wall property of protecting the core varied with the spray-drying and storage conditions. The OPR may be a goal directed and accurate description of the wall quality aiming at improving the stability of the carotene.

Acknowledgments This study was supported by the Hi-tech program of western Plan of Chinese Academy of Sciences (KGCX2-YW-509).

Conflict of interest None.

Compliance with Ethics Requirements This article does not contain any studies with human or animal subjects.

References

1. Aghbashlo M, Mobli H, Rafiee S, Madadlou A (2012) Optimization of emulsification procedure for mutual maximizing the encapsulation and exergy efficiencies of fish oil microencapsulation. Powder Technol 225:107–117. doi:10.1016/j.powtec.2012.03.040
2. Anwar SH, Kunz B (2011) The influence of drying methods on the stabilization of fish oil microcapsules: comparison of spray granulation, spray drying, and freeze drying. J Food Eng 105(2):367–378. doi:10.1016/j.jfoodeng.2011.02.047
3. Desobry SA, Netto FM, Labuza TP (1997) Comparison of spray-drying, drum-drying and freeze-drying for β-carotene encapsulation and preservation. J Food Sci 62(6):1158–1162. doi:10.1111/j.1365-2621.1997.tb12235.x
4. Frascareli EC, Silva VM, Tonon RV, Hubinger MD (2012) Effect of process conditions on the microencapsulation of coffee oil by spray drying. Food Bioprod Process 90(3):413–424. doi:10.1016/j.fbp.2011.12.002
5. Fuchs M, Turchiuli C, Bohin M, Cuvelier ME, Ordonnaud C, Peyrat-Maillard MN, Dumoulin E (2006) Encapsulation of oil in powder using spray drying and fluidised bed agglomeration. J Food Eng 75(1):27–35. doi:10.1016/j.jfoodeng.2005.03.047
6. Gharsallaoui A, Roudaut G, Chambin O, Voilley A, Saurel R (2007) Applications of spray-drying in microencapsulation of food ingredients: an overview. Food Res Int 40(9):1107–1121. doi:10.1016/j.foodres.2007.07.004
7. Kanakdande D, Bhosale R, Singhal RS (2007) Stability of cumin oleoresin microencapsulated in different combination of gum arabic, maltodextrin and modified starch. Carbohydr Polym 67(4):536–541. doi:10.1016/j.carbpol.2006.06.023
8. Kolanowski W, Ziolkowski M, Weißbrodt J, Kunz B, Laufenberg G (2006) Microencapsulation of fish oil by spray drying–impact on oxidative stability. Part 1. Eur Food Res Technol 222(3–4):336–342. doi:10.1007/s00217-005-0111-1
9. Labuza TP, Kaanane A, Chen JY (1985) Effect of temperature on the moisture sorption isotherms and water activity shift of two dehydrated foods. J Food Sci 50(2):385–392. doi:10.1111/j.1365-2621.1985.tb13409.x
10. Loksuwan J (2007) Characteristics of microencapsulated β-carotene formed by spray drying with modified tapioca starch, native

tapioca starch and maltodextrin. Food Hydrocoll 21(5–6): 928–935. doi:10.1016/j.foodhyd.2006.10.011
11. Nijdam JJ, Langrish TAG (2006) The effect of surface composition on the functional properties of milk powders. J Food Eng 77(4):919–925. doi:10.1016/j.jfoodeng.2005.08.020
12. Ochiai T, Shimeno H, Mishima K-i, Iwasaki K, Fujiwara M, Tanaka H, Shoyama Y, Toda A, Eyanagi R, Soeda S (2007) Protective effects of carotenoids from saffron on neuronal injury in vitro and in vivo. Biochim Biophys Acta 1770(4):578–584. doi:10.1016/j.bbagen.2006.11.012
13. Pérez-Alonso C, Báez-González JG, Beristain CI, Vernon-Carter EJ, Vizcarra-Mendoza MG (2003) Estimation of the activation energy of carbohydrate polymers blends as selection criteria for their use as wall material for spray-dried microcapsules. Carbohydr Polym 53(2):197–203. doi:10.1016/S0144-8617(03)00052-3
14. Qian C, Decker EA, Xiao H, McClements DJ (2012) Physical and chemical stability of β-carotene-enriched nanoemulsions: influence of pH, ionic strength, temperature, and emulsifier type. Food Chem 132(3):1221–1229. doi:10.1016/j.foodchem.2011.11.091
15. Rascón MP, Beristain CI, García HS, Salgado MA (2011) Carotenoid retention and storage stability of spray-dried encapsulated paprika oleoresin using gum arabic and soy protein isolate as wall materials. LWT Food Sci Technol 44(2):549–557. doi:10.1016/j.lwt.2010.08.021
16. Rocha GA, Fávaro-Trindade CS, Grosso CRF (2012) Microencapsulation of lycopene by spray drying: characterization, stability and application of microcapsules. Food Bioprod Process 90(1):37–42. doi:10.1016/j.fbp.2011.01.001
17. Rodea-González DA, Cruz-Olivares J, Román-Guerrero A, Rodríguez-Huezo ME, Vernon-Carter EJ, Pérez-Alonso C (2012) Spray-dried encapsulation of chia essential oil (*Salvia hispanica* L.) in whey protein concentrate-polysaccharide matrices. J Food Eng 111(1):102–109. doi:10.1016/j.jfoodeng.2012.01.020
18. Selim K, Tsimidou M, Biliaderis CG (2000) Kinetic studies of degradation of saffron carotenoids encapsulated in amorphous polymer matrices. Food Chem 71(2):199–206. doi:10.1016/S0308-8146(00)00156-4
19. Tonon RV, Grosso CRF, Hubinger MD (2011) Influence of emulsion composition and inlet air temperature on the microencapsulation of flaxseed oil by spray drying. Food Res Int 44(1):282–289. doi:10.1016/j.foodres.2010.10.018
20. Tsimidou M, Biliaderis CG (1997) Kinetic studies of saffron (*Crocus sativus* L.) quality deterioration. J Agric Food Chem 45(8):2890–2898. doi:10.1021/jf970076n
21. Turchiuli C, Fuchs M, Bohin M, Cuvelier ME, Ordonnaud C, Peyrat-Maillard MN, Dumoulin E (2005) Oil encapsulation by spray drying and fluidised bed agglomeration. Innov Food Sci Emerg Technol 6(1):29–35. doi:10.1016/j.ifset.2004.11.005
22. Van Calsteren M-R, Bissonnette MC, Cormier F, Dufresne C, Ichi T, LeBlanc JCY, Perreault D, Roewer I (1997) Spectroscopic characterization of Crocetin derivatives from *Crocus sativus* and *Gardenia jasminoides*. J Agric Food Chem 45(4):1055–1061. doi:10.1021/jf9603487
23. Wagner LA, Warthesen JJ (1995) Stability of spray-dried encapsulated carrot carotenes. J Food Sci 60(5):1048–1053. doi:10.1111/j.1365-2621.1995.tb06290.x
24. Wang Y, Ye H, Zhou C, Lv F, Bie X, Lu Z (2012) Study on the spray-drying encapsulation of lutein in the porous starch and gelatin mixture. Euro Food Res Technol 234(1):157–163. doi:10.1007/s00217-011-1630-6
25. Yang S, Mao X-Y, Li F-F, Zhang D, Leng X-J, Ren F-Z, Teng G-X (2012) The improving effect of spray-drying encapsulation process on the bitter taste and stability of whey protein hydrolysate. Euro Food Res Technol. doi:10.1007/s00217-012-1735-6
26. Zhang R, Qian Z-Y, Han X-Y, Chen Z, Yan J-L, Hamid A (2009) Comparison of the effects of Crocetin and Crocin on myocardial injury in rats. Chin J Nat Med 7(3):223–227. doi:10.1016/s1875-5364(09)60055-8